

***Smad1-Smad5* Ovarian Conditional Knockout Mice Develop a Disease Profile Similar to the Juvenile Form of Human Granulosa Cell Tumors**

Brooke S. Middlebrook, Karen Eldin, Xiaohui Li, Sujatha Shivasankaran, and Stephanie A. Pangas

Departments of Pathology (B.S.M., K.E., X.L., S.A.P.) and Obstetrics and Gynecology (S.S.), Baylor College of Medicine, Houston, Texas 77030

Granulosa cell tumors (GCTs) of the ovary are rare sex cord stromal tumors. Although generally indolent, GCTs recur, and if not diagnosed and treated in early stages, survival rates are significantly shortened. Very little is known regarding GCT etiology. Because of the low incidence of cases and lack of standard diagnostics, mouse models for granulosa cell tumors are a valuable tool for studying GCTs and provide models for developing diagnostic and treatment strategies. We recently developed a novel mouse model of metastatic granulosa cell tumors by genetic deletion of the bone morphogenetic protein signaling transcription factors (SMADs) in granulosa cells of the ovary. Histological and serum hormone analyses reveal that this mouse model most closely resembles the juvenile form of GCT. We further analyzed samples of human juvenile GCT (JGCT) for expression of anti-Müllerian hormone and activation of two major signaling pathways: TGF β /SMAD2/3 and wingless-related mouse mammary tumor virus integration site (Wnt)/ β -catenin. The TGF β family is active in mouse *Smad1-Smad5* double knockout tumors, and here we show that this pathway, but not the β -catenin pathway, is activated in samples of human JGCT. These data suggest that the SMAD family, possibly through disruption of SMAD1/5 or activation of SMAD2/3 may contribute to the pathogenesis of JGCT in humans. (*Endocrinology* 150: 5208–5217, 2009)

Sex cord stromal tumors are a rare ovarian cancer, comprising approximately 6–10% of cases. Granulosa cell tumors (GCTs) represent the largest category of sex-cord stromal tumors and share many characteristics with ovarian follicular granulosa cells including expression of the inhibin- α subunit (*INHA*) (1, 2) and anti-Müllerian hormone (AMH) (3). Whereas most GCTs are detected at early stages, recurrence occurs at a rate of approximately 43% (4), and 70% of GCT patients with recurrent disease die of the disease (5, 6). The mean time to relapse is 4–6 yr, but the disease-free interval can extend as long as 30 yr (5, 7, 8). Currently, Fédération Internationale de Gynécologie et d'Obstétrique (FIGO) stage is the only prognostic factor associated with poor survival (9–13). A more accurate prognostic marker for recurrence would benefit patient follow-up, although monitoring serum inhibin lev-

els (14, 15), or more recently AMH levels, has been suggested (16).

GCTs are classified into adult and juvenile forms. Adult granulosa cell tumors (AGCTs) occur predominantly in postmenopausal women with a median age of diagnosis between 50 and 54 yr (8). Juvenile granulosa cell tumors (JGCTs) occur within the first 2 decades of life and rarely occur past the age of 30 yr (17). Both forms of GCT can be hormonally active and may secrete estrogen, inhibins, AMH, and in some cases, androgens. In young children with GCTs, altered expression of hormones may result in isosexual precocious puberty, and in adults amenorrhea, infertility, or postmenopausal bleeding, depending on whether patients are pre- or postmenopausal. Key histological features distinguish adult from juvenile forms, including nuclear grooves (coffee bean nuclei) and Call-Ex-

ISSN Print 0013-7227 ISSN Online 1945-7170
Printed in U.S.A.

Copyright © 2009 by The Endocrine Society

doi: 10.1210/en.2009-0644 Received June 5, 2009. Accepted September 11, 2009.

First Published Online October 9, 2009

Abbreviations: AGCT, Adult granulosa cell tumor; AMH, anti-Müllerian hormone; BMP, bone morphogenetic protein; CV, coefficient variation; dKO, double conditional; GCT, granulosa cell tumor; INHA, inhibin- α subunit; JGCT, juvenile GCT.

ner bodies, the presence of which are pathognomonic of AGCT. Whether AGCT or JGCT have similar etiologies is unknown, and full molecular characterization of these types has not been carried out. However, a recently reported mutation in *FOXL2* is associated with most AGCT but only rarely in JGCT (18).

Natural and engineered mutations in mice have generated a number of mouse models that develop granulosa cell tumors. Several strains of inbred mice naturally develop GCTs, and whereas susceptibility loci have been identified (19–21), no definitive genetic mutations have been isolated from these strains. Mice with a deletion of *Inha*, encoding the α -subunit of inhibin, develop sex cord stromal tumors and die due to a cancer-cachexia like syndrome (22, 23). Mice with granulosa cell overexpression of β -catenin, a component of the WNT signaling pathway, develop a nonlethal form of GCT (24). Additionally, granulosa cell overexpression of simian virus 40 large T-antigen in mice gives a variable incidence of granulosa cell tumors (25, 26), and in one model, a 10% incidence of liver or lung metastases in older females (25).

We recently developed a mouse model for granulosa cell deletion of *Smad1* and *Smad5*, two transcription factors that signal for the bone morphogenetic proteins (BMPs) and AMH. Granulosa cell deletion of *Smad1* and *Smad5* results in granulosa cell tumors in mice early during sexual maturity (at least by 8 wk of age). These mice are initially subfertile and subsequently become infertile (27). This phenotype occurs in 100% of the conditional knockout mice, and approximately 80% develop peritoneal and lymphatic metastases by 8 months of age (27). Expression profiling and immunohistochemical analysis indicate activation of the SMAD-2/3 pathway and disruptions in signaling by the TGF β family (27) in these tumors. In our current study, we further characterize this mouse model and show that they are similar to human JGCT. Furthermore, we demonstrate that human JGCTs contain similarities to the *Smad1-Smad5* double conditional (dKO) mouse model, such as activation of the TGF β /SMAD2/3 pathway. Based on these studies of mouse and human GCTs, the *Smad1-Smad5* dKO mouse model is a suitable candidate model for understanding the pathogenesis of JGCT and exploring potential future diagnostic markers and treatment regimens.

Materials and Methods

Animals

Experimental animals were maintained in accordance with the National Institutes of Health Guide for the Care and Use of Laboratory animals using Institutional Care and Use Committee-approved protocols at Baylor College of Medicine. The *Smad1*,

Smad5, and *Amhr2cre* conditional and null alleles and generation of *Smad1-Smad5* dKO lines have been described in detail elsewhere (27). Mice in this study were maintained on a C57BL/6J;129S5/SvEvBrd mixed hybrid background and genotyped as described (27). Single conditional knockouts have normal fertility and do not develop tumors as described (27). *Smad1-Smad5* dKO mice were of the genotypes: *Smad1*^{flox/flox} *Smad5*^{flox/flox} *Amhr2*^{cre/+}, *Smad1*^{flox/-} *Smad5*^{flox/flox} *Amhr2*^{cre/+}, or *Smad1*^{flox/flox} *Smad5*^{flox/-} *Amhr2*^{cre/+}. No differences were noted for mice with either three floxed or four floxed *Smad* alleles. Control mice were the same genotype as the experimental mice except that they were negative for the *Cre* allele (*Amhr2*^{+/+}).

Human samples

Archived, deidentified, formalin-fixed, paraffin-embedded JGCT samples from surgical resections were acquired from the Department of Pathology's Tissue Bank at Texas Children's Hospital (Houston, TX). Tissues were treated in accordance with Baylor College of Medicine Institutional Review Board approval and a waiver of consent was approved (Institutional Review Board no. H-23139). A total of nine samples of JGCTs were examined: five ovarian JGCT, two testicular JGCT, and two malignant implants from a Fédération Internationale de Gynécologie et d'Obstétrique stage IIIB patient. The ages of the JGCT patients ranged from 3 months to 15 yr, with a mean age of 5.7 yr. Pathological assessment was performed by the Department of Pathology at Texas Children's hospital.

Mouse serum and tissue collection

Mice were anesthetized by isofluorane inhalation then euthanized by cervical dislocation. Tissues were fixed in 10% neutral-buffered formalin, processed, and embedded in paraffin at the Baylor College of Medicine Pathology Core Histology Facility using standard techniques. Blood was collected from anesthetized mice by cardiac puncture and serum collected in Microtainer serum separator tubes (Becton Dickinson, Franklin Lakes NJ) and frozen at -20°C until assayed. Serum was collected from random cycling females, which were group housed.

Hormone assays

FSH, LH, estradiol, inhibin A, and inhibin B measurements were made by the University of Virginia Ligand Core Facility (Specialized Cooperative Centers Program in Reproductive Research National Institute of Child Health and Human Development/National Institutes of Health U54 HD28934) as described (28). Assay information including inter- and intracoefficient variation (CV) is available (<http://www.healthsystem.virginia.edu/internet/crr/ligand.cfm>). FSH values in cycling wild-type mice range from approximately 5 ng/ml at proestrus, peak at approximately 25 ng/ml at estrus, and then return to 5–10 ng/ml at metestrus and diestrus (29). Serum AMH was measured by ELISA (Diagnostic Systems Laboratories, Webster, TX) using the manufacturer's protocol. This kit has a sensitivity of 17 pg/ml, an interassay CV of 6.7–8% and intraassay CV of 2.4–4.6%. It has been reported that peak estrus levels of AMH levels in wild-type mice are less than 45 ng/ml (29). When necessary, serum samples were diluted in PBS to fall within the detectable range. For statistical purposes, values that fell below the threshold value were given the threshold value.

Histology and immunohistochemistry

Formalin-fixed, paraffin embedded sections were processed by the Baylor College of Medicine Core Histology Laboratory for histology. Immunohistochemistry was performed as described (30). The following antibody dilutions were used: goat anti-AMH antibody (C-20; Santa Cruz Biotechnology, Santa Cruz, CA) 1:2500 (mouse) or 1:100 (human); rabbit anti-phosphohistone H3 (Ser10; Upstate Laboratories, Lake Placid, NY) 1:200; rabbit anti-phospho-SMAD2/3 (Ser465/467; Cell Signaling Technologies, Beverly, MA; mouse anti-inhibin- α (R1 monoclonal; Serotec, Oxford, UK) 1:15; mouse anti- β -catenin (clone 14; BD Transduction Laboratories, San Diego, CA) 1:75 to 1:125. The mouse-on-mouse immunodetection kit (Vector Laboratories, Burlingame, CA) was used for immunohistochemistry on mouse tissue when using mouse monoclonal antibodies. For mouse tissues, immunohistochemistry was performed on a minimum of four independent samples in duplicate. Negative controls (no primary antibody) were run in parallel for all experiments and showed little to no immunoreactivity. Mitotic index was calculated as described (31). Briefly, the number of mitoses in 10 high-power fields ($\times 40$) was counted in three areas of each sample and averaged. A final mean \pm SE was calculated for four independent samples of *Smad1-Smad5* dKO tumors from mice at 32–36 wk of age.

Statistical analysis

Statistical analyses were performed using SPSS (version 16.0; Chicago, IL). Serum hormone values were log transformed before statistical analysis. Student's *t* test was used for comparisons between two groups. Statistical significance was set at $\alpha = 0.05$. Kaplan Meier curves were generated for survival studies and statistical significance determined by the log-rank test.

Results

Histology of *Smad1-Smad5* dKO tumors is similar to JGCT

Previously we generated dKO mice with granulosa cell deletion of the BMP signaling SMADs, SMAD1 and SMAD5, using *Amhr2cre*-mediated recombination (27). To further characterize this line and establish the lethality of phenotype, we aged control (*cre* negative littermates; $n = 9$) and *Smad1-Smad5* dKO ($n = 9$) females for 8 months. All of the control mice were alive at the end of 8 months, but only 33% of *Smad1-Smad5* dKO females survived to 32 wk, with 50% survival at approximately 29 wk of age (Fig. 1A). GCTs from *Smad1-Smad5* dKO mice are similar to JGCTs because they lacked nuclear grooves and only infrequently contained Call-Exner bodies (Table 1 and Fig. 1B). The mitotic index has been reported to be higher in JGCTs (average of seven per 10 high power field) than AGCTs (17). Brisk mitotic activity was apparent in *Smad1-Smad5* dKO tumors and the average mitotic index (number of mitotic figures in 10 high power fields) of GCTs from *Smad1-Smad5* dKO mice was 19.1 ± 5.5 ($n = 4$). In addition, *Smad1-Smad5* dKO tumors stained pos-

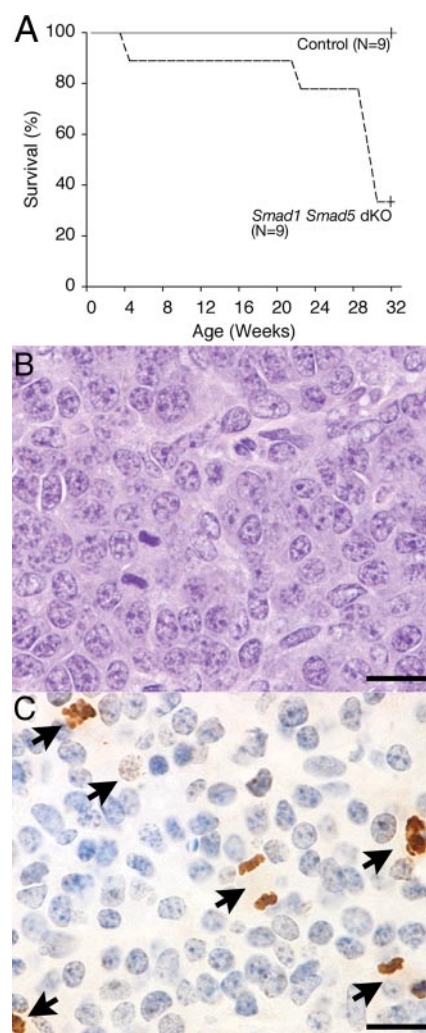


FIG. 1. A, Survival curves for control and *Smad1-Smad5* dKO mice over an 8-month period. Survival is significantly different between genotypes ($P < 0.01$). In the *Smad1-Smad5* dKO mice, 33% of the mice survive to 32 wk of age, whereas all the control mice are viable. B and C, Histology of *Smad1-Smad5* dKO tumors. B, Tumors lack the coffee bean nuclear grooves characteristic of AGCTs. Hematoxylin and eosin staining of a tumor from a 32-wk dKO female is shown. C, Mitotic cells as demonstrated by phosphohistone H3 immunostaining (brown) (arrows) are abundant in *Smad1-Smad5* dKO tumors. Cell nuclei are blue. Tumor is from a 35-wk-old female. Both images at $\times 780$ magnification. Scale bar, 20 μ m.

itively for phosphohistone H3 (Fig. 1C), a marker for late G_2 and M phase.

Serum hormones profiles are altered in *Smad1-Smad5* dKO mice

Patients with GCTs may have altered serum profiles of estradiol, FSH, LH, inhibin, and AMH (Table 1 and references therein). Hormone analysis of *Smad1-Smad5* dKO mice indicated that serum levels of FSH were significantly suppressed in *Smad1-Smad5* dKO mice, whereas serum LH and estradiol were not significantly changed from the controls (Table 2). Inhibins negatively regulate pituitary FSH, and because we had previously determined

TABLE 1. Comparison of adult GCTs, juvenile GCTs, and tumors from *Smad1-Smad5* dKO mice

Characteristic	Adult GCTs (Hu)	Juvenile GCTs	<i>Smad1-Smad5</i> dKO
Histological features			
Grooved nuclei	Present/frequent	Absent	Absent
Call-Exner bodies	Present/frequent	Absent	Rare to absent
Mitotic index	Low	High	High
Serum hormone profile			
Estradiol	Increased but variable	Increased	Increased but variable
FSH	Decreased (54, 55)	Very low (56)	Low to undetectable
LH	Increased (54)	Very low (56)	No change
Inhibin A (dimeric)	Moderate increase (14)	ND	Increased
Inhibin B (dimeric)	Dramatic increase (14)	Increased (56)	Increased but variable
AMH	Increased (3, 34, 35)	Increased (36)	Increased

ND, No data; Hu, human.

that *Smad1-Smad5* dKO tumors were immunopositive for the inhibin- α subunit (27), we measured serum levels of inhibin A and inhibin B. Inhibin A was significantly elevated ($P < 0.001$) in *Smad1-Smad5* dKO mice with tumors compared with control mice (Fig. 2A). Whereas the mean level of inhibin B was elevated, its levels were variable and failed to make the cutoff for statistical significance ($P = 0.07$) (Fig. 2B).

AMH is expressed in *Smad1-Smad5* dKO tumors and JGCTs

We measured AMH localization and serum levels in ovaries and tumors from *Smad1-Smad5* dKO mice and their controls. AMH is expressed in granulosa cells of growing follicles in the mouse ovary in preantral stages but declines in expression in preovulatory follicles with expression remaining only within cumulus cells (Fig. 3A) (32, 33). Like its controls, *Smad1-Smad5* dKO ovaries contain AMH immunoreactivity in preantral follicles; however, granulosa cells in antral follicles inappropriately retain patchy expression of AMH, suggesting that the granulosa cell differentiation pattern has been altered (Fig. 3B). AMH continues to be expressed in *Smad1-Smad5* dKO primary tumors (Fig. 3C) and tumor cells as they metastasize outside the ovary (Fig. 3B, D and E). In addition, serum AMH levels were significantly elevated in *Smad1-Smad5* dKO mice (Fig. 2C).

We further analyzed AMH expression in samples of ovarian JGCTs ($n = 5$), testicular JGCTs ($n = 2$), and

malignant implants ($n = 2$ from one ovarian JGCT patient). AMH is reported to be expressed at variable levels with patchy expression in AGCTs or JGCTs (3, 34–36). Of the five ovarian JGCT samples, three showed low to background staining (data not shown), and two showed weak but patchy immunoreactivity (the strongest of the ovarian JGCTs is shown in Fig. 4A). However, the highest level of immunoreactivity was demonstrated in the JGCT of the testis samples (Fig. 4E) and in both malignant implant samples from a patient with an ovarian JGCT (Fig. 4C).

An active SMAD2/SMAD3 but not β -catenin pathway is present in JGCT

The signaling pathways that contribute to human GCT tumor development are not well understood. β -Catenin has been shown to be active (*i.e.* shows nuclear localization) in a small subset of human GCTs (one of six samples of an unspecified type) and a large number of equine GCT (14 of 18) (24). Granulosa cells in mouse ovaries expressed β -catenin, with the highest expression level in preantral follicles (supplemental Fig. S1A, published as supplemental data on The Endocrine Society's Journals Online web site at <http://endo.endojournals.org>). In *Smad1-Smad5* dKO tumors, β -catenin is expressed similar to control preovulatory granulosa cells, and its localization is predominantly cytoplasmic or membranous with few cells showing nuclear staining (supplemental Fig. S1). We also examined the immunolocalization of β -catenin in our samples of human JGCTs. All samples (five ovarian, two testicular, two malignant implants) showed positive immunoreactivity, but the localization was confined to the cytoplasm/membrane (Fig. 5). Although the number of human cases examined is few, our studies suggest that the activation of the WNT/ β -catenin pathway does not play a critical role in JGCTs or the *Smad1-Smad5* dKO mouse model.

Loss of the inhibin- α subunit causes sex cord stromal tumors in mice with full penetrance (22). Because dimeric inhibin can no longer be produced due to deletion of the α -subunit, gonadal tumor development in inhibin- α mice

TABLE 2. Concentrations of estradiol, FSH, and LH in serum of control mice and *Smad1-Smad5* dKO mice

Hormone assay	Control	n	<i>Smad1-Smad5</i> dKO	n	P value
Estradiol (pg/ml)	19.6 \pm 2.0	18	30.5 \pm 6.7	6	0.101
FSH (ng/ml)	13.8 \pm 2.6	22	2.7 \pm 0.4	11	0.000
LH (ng/ml)	0.5 \pm 0.1	17	0.3 \pm 0.1	5	0.531

Concentrations are given as mean \pm SEM. Significant differences between the means were found for FSH alone, whereas estradiol levels showed an increased trend. n, Number of animals measured.

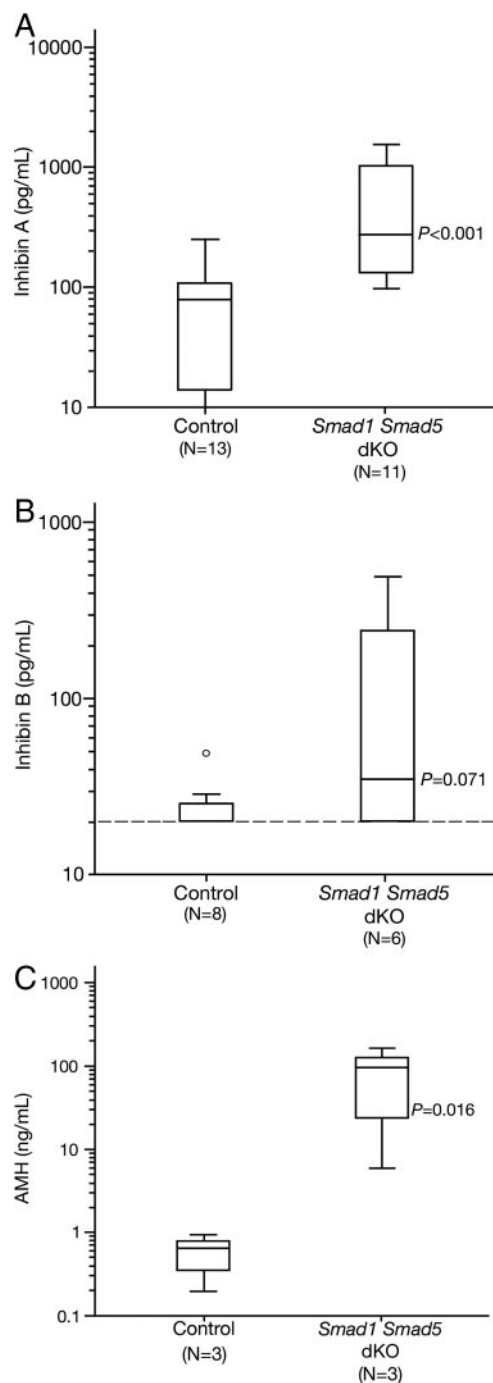


FIG. 2. Serum inhibin and AMH levels in control and *Smad1-Smad5* dKO mice. Graph shows box and whisker plots, with each box representing the 75th and 25th percentile with the median value indicated as a solid vertical line. Whiskers are the highest and lowest values not including outliers. A, Inhibin A values significantly increase in *Smad1-Smad5* dKO mice compared with controls ($P < 0.001$). B, There is an increased trend in inhibin B values, which is not statistically significant ($P = 0.071$). The circle represents the outlier sample (3 times the interquartile range). The dashed line represents the detection limit of the inhibin B assay. N, Number of animals assayed. C, AMH values significantly increase in *Smad1-Smad5* dKO mice over the controls ($P = 0.016$).

has been partly attributed to activin activity (37). Activin signals through SMAD2 and SMAD3, which accumulate in the nucleus when phosphorylated at the carboxyl ter-

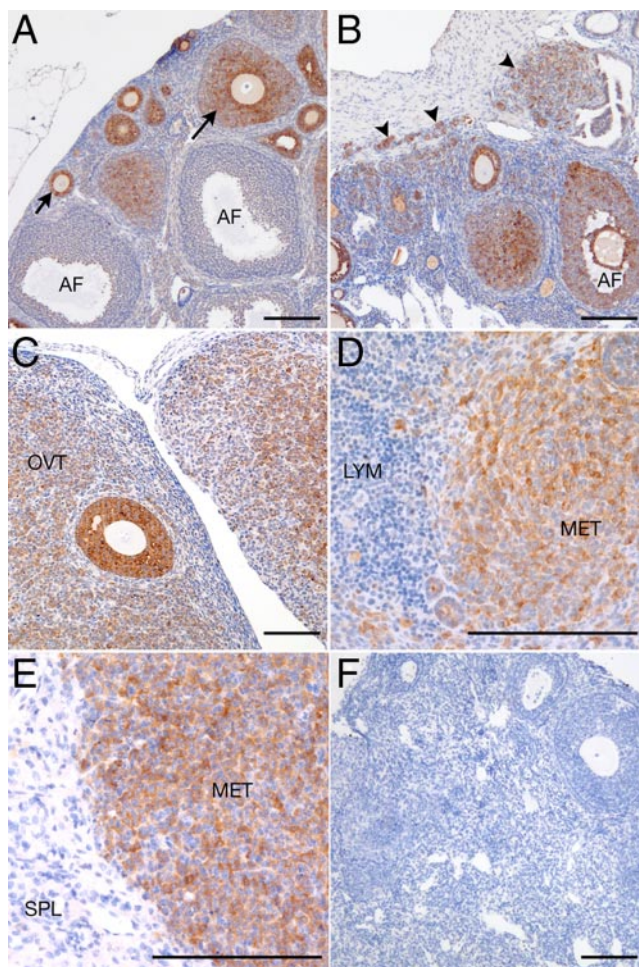


FIG. 3. Immunohistochemistry for AMH in control and *Smad1-Smad5* dKO ovaries and *Smad1-Smad5* dKO tumors and metastases. A, AMH immunoreactivity of 8-wk control ovaries. AMH is expressed in granulosa cells of growing follicles (arrows) but not antral follicles (AF). B, AMH immunoreactivity in 8-wk *Smad1-Smad5* dKO ovaries, but its expression is not down-regulated in antral follicles (AF). Additional immunoreactivity is seen in tumor cells in the fat pad and oviduct (arrowheads). AMH immunoreactivity is evident in primary tumors (C) (OVT) and metastases (MET), shown for a lymph node (LYM) (D) and spleen (SPL) (E). F, Negative controls showed little immunoreactivity. Brown indicates immunoreactivity to AMH, and cell nuclei counterstained with hematoxylin (blue). Scale bar in all panels, 100 μ m.

mini. In rodent ovaries, SMAD2 and SMAD3 are detected in granulosa cells of small growing follicles at levels greater than preovulatory follicles (38); in human ovaries, SMAD2 is expressed preantral and antral stage granulosa cells, although the cytoplasmic *vs.* nuclear localization is variable (39). In support of an active SMAD2/3 pathway in the inhibin- α null mouse model, tumors from adult *Inha*^{-/-} females were strongly positive for nuclear C-terminal phospho-SMAD2/3 staining (Fig. 6A).

It is unknown whether an active SMAD2/3 pathway is a common feature of GCTs. Previous data demonstrate that all *Smad1-Smad5* dKO tumors (Fig. 6B) (27) are strongly immunoreactive for phospho-SMAD2/3. We further investigated phospho-SMAD2/3 immunolocalization

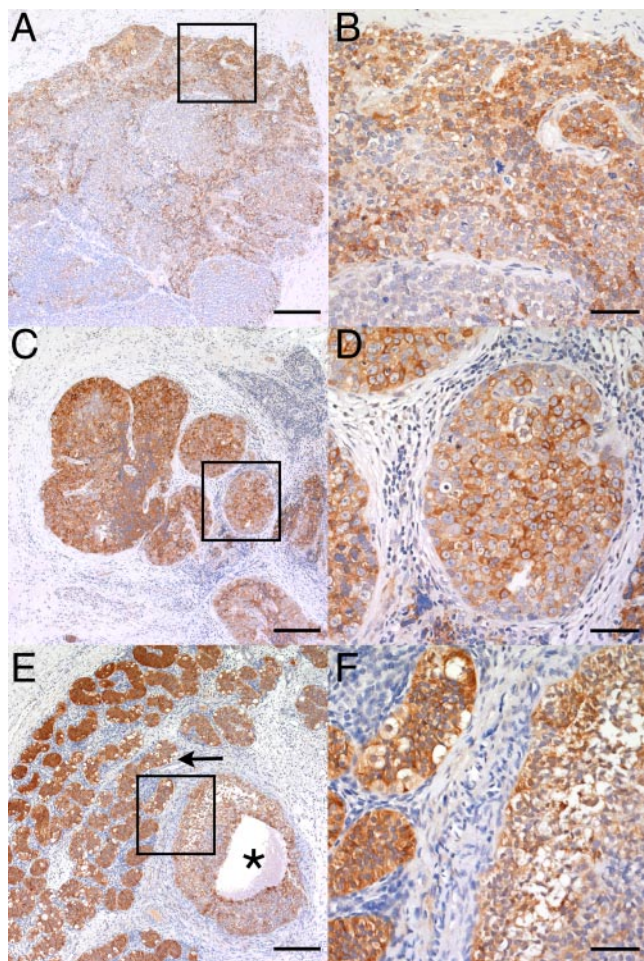


FIG. 4. Immunohistochemistry for AMH in samples of human JGCT and malignant implants. A, Immunoreactivity in a JGCT of the ovary from a 15-yr-old patient. Boxed region is shown at higher magnification in B. This sample demonstrates the highest degree of AMH immunoreactivity of all of the female ovarian JGCT samples. C, Immunoreactivity in a stage IIIB malignant JGCT sample from a 14-yr-old female. Boxed region is shown at a higher magnification in D. E, Immunoreactivity in a JGCT from a testis of a 3-month-old infant. Boxed region is shown at a higher magnification in F. Arrow indicates AMH-positive Sertoli cells in seminiferous tubules. Asterisk indicates AMH-positive cells in the JGCT arranged in a follicle-like pattern. Secondary antibody only control staining (not shown) demonstrated little to no background staining. In all panels, brown indicates positive immunoreactivity to AMH, and nuclei are counterstained with hematoxylin (blue). Magnification (A, C, and E), $\times 50$. Scale bar, 200 μm . Magnification (B, D, and F), $\times 200$. Scale bar, 50 μm .

in samples of JGCTs. All samples of ovarian and testicular JGCTs, as well as the ovarian GCT implants, had readily detectable nuclear immunostaining for phospho-SMAD2/3 (Fig. 6, C–F), suggesting that the SMAD2 and/or SMAD3 is active in JGCTs and thus may play a role in JGCT tumor physiology.

Discussion

Mouse models are invaluable tools for understanding human disease and critical for research into rare diseases in

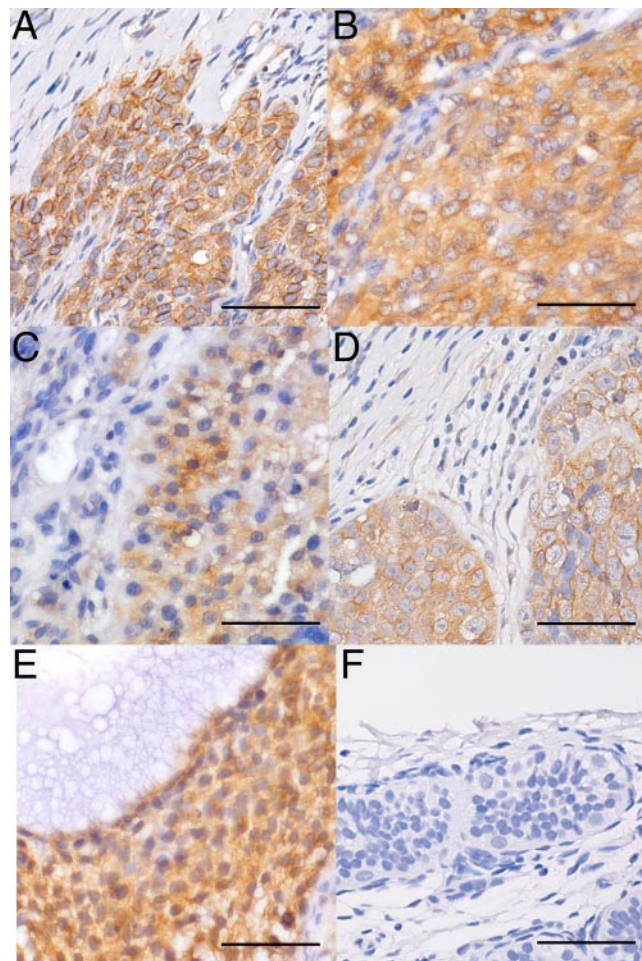


FIG. 5. Immunohistochemistry for β -catenin in samples of human JGCTs and malignant implants. β -Catenin in its inactive state is localized to the plasma membrane and active when nuclear. The majority of β -catenin staining in all JGCTs was membranous or cytoplasmic. A, Immunoreactivity in an ovarian JGCT from a 2-yr-old patient. B, Immunoreactivity in an JGCT of the ovary from a 3-yr-old patient. C, Immunoreactivity in a JGCT of the ovary from a 1-yr-old patient, who was reported to have multiple tumor syndrome. The sample demonstrated the least immunoreactivity of all samples tested. D, Immunoreactivity in a stage IIIB malignant JGCT sample from a 14-yr-old female. E, Immunoreactivity in a JGCT from a testis of a 3-month-old infant. F, Secondary antibody only control staining of same sample as shown in panel E, demonstrating little to no background staining. In all panels, brown indicates positive immunoreactivity to β -catenin, and nuclei are counterstained with hematoxylin (blue). Magnification at 400 \times , scale bar in all panels, 50 μm .

which patient populations and tissue samples are limited. GCTs are a rare ovarian cancer, and no definitive etiology is known for either JGCTs or AGCTs. Several mouse models develop GCTs, including deletion of inhibin- α , conditional overexpression in the ovary of β -catenin, and conditional deletion in the ovary of the BMP/AMH signaling SMADs, *Smad1* and *Smad5* (22, 24, 27). None of these mouse models is a phenocopy of the each other because each develops GCTs with a unique pattern, natural history, and histology and validates the notion that disruptions in multiple signaling pathways can lead to GCT for-

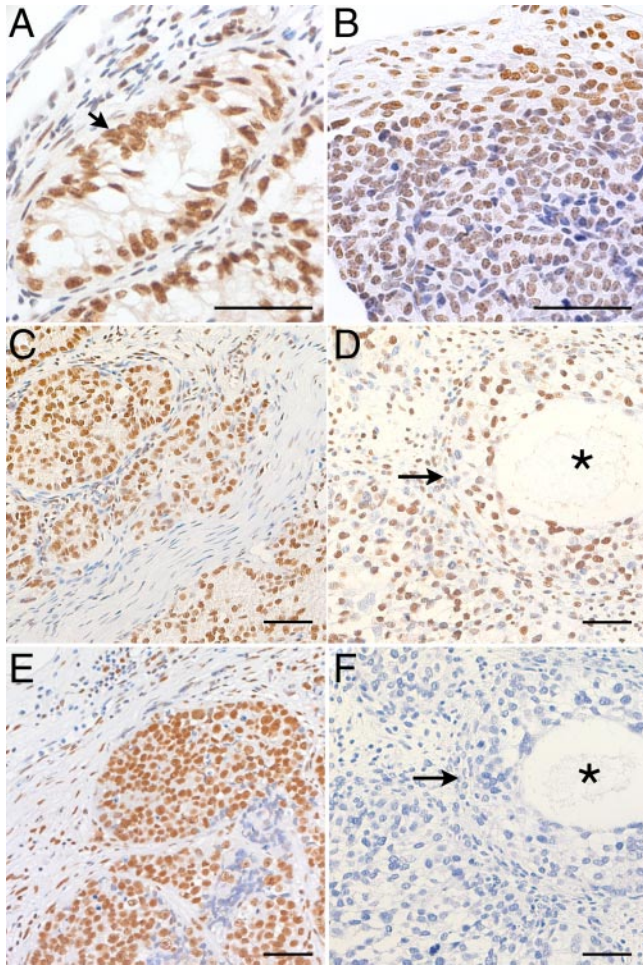


FIG. 6. Immunohistochemistry for active (phospho) SMAD2/3 in knockout mice (A and B) and human JGCTs and metastatic implants (C–F). A, Immunoreactivity in an ovarian tumor from a 25-wk-old adult *Inha*^{−/−} null mouse showing nuclear localization in cells within a Sertoli tubule-like structure (arrow). B, Phospho-SMAD2/3 immunoreactivity in a GCT from a 32-wk-old *Smad1*^{flox/flox} *Smad5*^{flox/flox} *Amhr2*^{cre/+} dKO mouse. C, Immunoreactivity in a JGCT of the ovary from a 2-yr-old patient. D, Immunoreactivity in a JGCT of the ovary from a 1-yr-old patient with multiple tumor syndrome. As with β -catenin (Fig. 5C), this sample showed the least immunoreactivity in tumor cells. E, Immunoreactivity in a malignant implant from a 14-yr-old patient with stage IIIB JGCT. F, Negative (IgG) control with same tissue as in D. D and F also show the remains of a secondary follicle (arrow) with abnormal and disordered granulosa cells but containing an oocyte (asterisk). In all panels, brown indicates positive immunoreactivity to phospho-SMAD2/3, and tissues are counterstained with hematoxylin (blue). Scale bar (all panels), 50 μ m.

mation. However, the role that any of these signaling pathways play in the pathogenesis of GCT in humans is unclear, as is whether they share a common mechanism(s) leading to GCT.

Deletion of *Smad1* and *Smad5* leads to granulosa cell tumor development in young mice (27). We extend these studies by examining their histological and hormonal profile, with the goal of establishing the similarity to human GCTs. JGCTs and AGCTs in humans are distinguished mostly by age at presentation and histological criteria

(17). The *Smad1-Smad5* dKO mice develop tumors while very young and at a time when they should be reproductively competent. In addition, the histological pattern of few to no Call-Exner bodies, cell nuclei lacking grooves, and a high mitotic index and proliferation rate suggest that the *Smad1-Smad5* dKO tumors most similarly reflect JGCTs. Future studies on the expression profiles of tumors from *Smad1-Smad5* dKO mice may reveal highly expressed genes and altered signal transduction pathways and thus provide suitable candidates for analysis in human GCT, as we also now show for activation of the SMAD2/3 pathway (see below).

Granulosa cells secrete a number of hormones, including inhibin and AMH, which may be used to track GCT development and/or recurrence. Upon tumor resection, inhibin levels fall and increase again when tumors recur (40). Inhibin B has been suggested to be the major form of inhibin secreted by AGCTs (14). Inhibin may have a limited utility. In JGCTs because of fluctuations in serum inhibin levels in premenopausal women (41). The hormonal profile of *Smad1-Smad5* dKO mice is similar to human GCTs, with decreased or undetectable levels of serum FSH and increases in serum inhibins. GCTs from *Smad1-Smad5* dKO mice express the subunits necessary for inhibin A and inhibin B production (27) (data not shown). In contrast to inhibin A, serum inhibin B levels were more variable, although trended toward increased levels, with some *Smad1-Smad5* dKO mice showing barely detectable levels and others as much as a 25-fold higher level than controls. It is unclear why these differences arise, and studies are ongoing to try to understand this phenomenon.

AMH and JGCTs

AMH is an additional marker proposed for GCTs (16, 35, 42). Granulosa and Sertoli cells produce AMH, depending on developmental stage. AMH is highly expressed in growing follicles but is down-regulated in pre-ovulatory follicles (43, 44). *Smad1* and *Smad5* deletion in the mouse ovary has no effect on AMH expression in small growing follicles. However, AMH continues to be expressed in granulosa cells of larger antral follicles of *Smad1-Smad5* dKO ovaries, suggesting that granulosa cell differentiation is disrupted. AMH is also expressed in tumor cells from *Smad1-Smad5* dKO mice and is maintained in cells as they spread outside the ovary. Interestingly, the lack of AMH expression in human GCTs associates with a greater growth potential of these tumors (31); therefore, deletion of *Smad1* and *Smad5* may create an analogous signaling pattern (*i.e.* there is little AMH to restrict growth of human GCTs; likewise, AMH is unable to signal in *Smad1 Smad5* dKO mice due to their deletion).

Our data support the hypothesis that AMH functions as a repressor of granulosa cell or GCT growth (45, 46). Other studies have shown a suppressive effect of AMH on cancer cell lines with intact AMH signaling components, including epithelial ovarian cancer (47, 48). In addition, activin via SMAD2/3 has shown a growth-promoting effect on some epithelial ovarian cancers (49–51). Thus, it is possible that SMAD1 and SMAD5 have important roles as tumor suppressors, inhibiting growth by regulating the activin/SMAD2/3 pathways, although the mechanism by which this occurs is unknown. Our data further indicate that using AMH as a neoadjuvant or adjuvant in cancer treatments (52) requires an intact and fully functional BMP-SMAD pathway to be successful. Cells that do not respond appropriately to growth inhibition by AMH may have become insensitive due to loss or misregulation of the appropriate receptors, SMADs, and/or coregulators.

The expression pattern of AMH in samples of human GCTs has been described (3). That study, which included seven ovarian JGCT, six ovarian AGCTs, and three extraovarian metastases demonstrated that JGCTs and AGCTs as well as extraovarian implants show a heterogeneous expression pattern with areas of intense or weak AMH immunoreactivity; even though AMH-positive cells remain a minority percentage, all cases were positive (3). In our current study, we added an additional five cases of JGCTs, two extraovarian implants, and two JGCTs of the testis, whose expression of AMH is previously uncharacterized. For ovarian JGCTs, several of our samples demonstrated negative staining, whereas some had patchy though weakly positive staining and were generally much weaker than the male JGCTs. The negative staining of some of our samples may reflect the heterogeneous nature of the tumors (3), or there may be a wide range of expression patterns in JGCTs. Although representing only one patient, the extraovarian implants showed a highly positive immunoreactivity to AMH. However, conclusions regarding AMH expression levels in metastases compared with the primary tumor cannot be made currently due to lack of additional implant samples in our tissue bank. The testicular JGCT samples also showed very strong immunostaining for AMH. These data are in contrast to testicular Sertoli cell tumors, which have very few AMH-positive cells (3). Although preliminary, AMH expression appears to be a good marker for distinguishing Sertoli tumors and GCTs of the testis, similar to AMH's ability to distinguish ovarian granulosa cell tumors from other sex cord stromal tumors of the ovary (3).

Activated signaling pathways and JGCTs

The β -catenin overexpression mouse model (24) and the *Smad1-Smad5* dKO mouse model (27) are two of the

most recent mouse models that show GCT development, and the importance of either of these signaling pathways has yet to be established in human GCTs. Mice conditionally mutant for phosphatase and tensin homolog (PTEN) that also overexpress β -catenin show GCT development at an accelerated rate, although phosphatase and tensin homolog (PTEN) mutations or altered expression is not associated with GCTs (53). Expression and nuclear localization (indicating activation) of β -catenin was originally described in one of six samples of GCT, although their division into adult or juvenile was not reported (24). We additionally studied the localization of β -catenin by immunohistochemistry in five samples of ovarian JGCT, although all samples studied showed membranous or cytoplasmic localization. In addition, two samples of implants and two testicular JGCTs also showed in general the expression pattern of membranous/cytoplasmic restriction. It is possible that the differences between these two studies reflect differences between AGCTs and JGCTs, and follow-up studies with additional samples will be necessary. It is also possible that activation of the β -catenin pathway is a rare, although nevertheless, important event in GCT development.

The TGF β family has important roles in tumorigenesis and metastasis in many cancer cell types. Whether the TGF β or BMP SMAD pathways play a role in the physiology of human GCTs is unknown. The full penetrance of GCT development and severity of the phenotype in the *Smad1-Smad5* dKO mice suggest that the BMP-SMADs may act as tumor suppressors in granulosa cells (27), thus identifying this as a candidate pathway for analysis in JGCTs. Our initial studies on *Smad1-Smad5* dKO mice indicated that the TGF β pathway and TGF β target genes were altered and that phosphorylated and nuclear forms of SMAD2 and SMAD3 were present in *Smad1-Smad5* dKO primary tumors and their metastases. We extend this study to show that similarly, GCTs derived from inhibin- α knockout mice have activation of SMAD2/3, suggesting the possibility of a shared mechanism between these mouse models in granulosa cell tumorigenesis. Furthermore, analysis of samples of human ovarian and testicular JGCT, as well as the ovarian JGCT implants, demonstrate a previously uncharacterized activation of the SMAD2/3 pathway in JGCTs. The functional significance of an active SMAD2/3 pathway in JGCT is unknown, although under further investigation.

Future directions

The phenotype of the *Smad1-Smad5* dKO mouse most closely resembles JGCT at a physiological as well as histological level. Understanding the mechanism underlying tumor development in these mice may uncover a similar

pathophysiology operating in JGCTs. For example, our initial analysis implicated the TGF β SMAD2/3 pathway as being active in *Smad1-Smad5* dKO tumors, and this has led to the novel discovery described herein of a similar SMAD2/3 activation in human JGCTs of both ovarian and testicular origin. A crucial next step will be to understanding the function and possible dysregulation of these signaling pathways in human GCTs.

Acknowledgments

We thank Drs. Elizabeth Robertson (University of Oxford, Oxford, UK) for the *Smad1* mice, Richard Behringer (University of Texas M. D. Anderson Cancer Center, Houston, TX) for *Ambr2cre* mice, Martin Matzuk (Baylor College of Medicine, Houston, TX) for the *Smad5* null mice, and Danny Huylebroeck, An Zwijsen, and Lieve Umans (University of Leuven, Leuven, Belgium) for *Smad5* floxed mice. We thank Dr. Martin Matzuk and Ankur Nagaraja (Baylor College of Medicine) for providing inhibin- α null tumor sections and Drs. Martin Matzuk, Matt Anderson, and Michelle Myers (Baylor College of Medicine) for critical reading of the manuscript. We thank Dr. Milton Finegold (Baylor College of Medicine) for assistance with JGCT collection. We thank the University of Virginia Ligand Core Facility (National Institute of Child Health and Human Development/National Institutes of Health U54 HD28934) for hormone assays.

Address all correspondence and requests for reprints to: Stephanie A. Pangas, Ph.D., Assistant Professor, Department of Pathology, One Baylor Plaza, Houston, Texas 77030. E-mail: spangas@bcm.edu.

This work was supported by a Burroughs Wellcome Career Award, a Dan L. Duncan Scholar Award (Baylor College of Medicine), and a grant from the Caroline Wiess Law Fund for Molecular Medicine and L. E. and Josephine S. Gordy Memorial Cancer Research Fund in the Biomedical Sciences (to S.A.P.).

Disclosure Summary: The authors have nothing to disclose.

References

- Arora DS, Cooke IE, Ganesan TS, Ramsdale J, Manek S, Charnock FM, Groome NP, Wells M 1997 Immunohistochemical expression of inhibin/activin subunits in epithelial and granulosa cell tumours of the ovary. *J Pathol* 181:413–418
- Fuller PJ, Chu S, Jobling T, Mamers P, Healy DL, Burger HG 1999 Inhibin subunit gene expression in ovarian cancer. *Gynecol Oncol* 73:273–279
- Rey R, Sabourin JC, Venara M, Long WQ, Jaubert F, Zeller WP, Duvillard P, Chemes H, Bidart JM 2000 Anti-Mullerian hormone is a specific marker of Sertoli- and granulosa-cell origin in gonadal tumors. *Hum Pathol* 31:1202–1208
- Schouli J, Drescher FS, Mustea A, Elling D, Friedmann W, Kühn W, Nehmzow M, Opri F, Klare P, Dietel M, Lichtenegger W 2004 Granulosa cell tumor of the ovary: 10 years follow-up data of 65 patients. *Anticancer Res* 24:1223–1229
- Colombo N, Parma G, Zanagnolo V, Insinga A 2007 Management of ovarian stromal cell tumors. *J Clin Oncol* 25:2944–2951
- Amsterdam A, Selvaraj N 1997 Control of differentiation, transformation, and apoptosis in granulosa cells by oncogenes, oncoviruses, and tumor suppressor genes. *Endocr Rev* 18:435–461
- Malmström H, Högborg T, Risberg B, Simonsen E 1994 Granulosa cell tumors of the ovary: prognostic factors and outcome. *Gynecol Oncol* 52:50–55
- Schumer ST, Cannistra SA 2003 Granulosa cell tumor of the ovary. *J Clin Oncol* 21:1180–1189
- Björkholm E, Silfverswärd C 1981 Prognostic factors in granulosa-cell tumors. *Gynecol Oncol* 11:261–274
- Evans 3rd AT, Gaffey TA, Malkasian Jr GD, Annegers JF 1980 Clinicopathologic review of 118 granulosa and 82 theca cell tumors. *Obstet Gynecol* 55:231–238
- Stenwig JT, Hazekamp JT, Beecham JB 1979 Granulosa cell tumors of the ovary. A clinicopathological study of 118 cases with long-term follow-up. *Gynecol Oncol* 7:136–152
- Auranen A, Sundström J, Ijäs J, Grénman S 2007 Prognostic factors of ovarian granulosa cell tumor: a study of 35 patients and review of the literature. *Int J Gynecol Cancer* 17:1011–1018
- Mom CH, Engelen MJ, Willemse PH, Gietema JA, ten Hoor KA, de Vries EG, van der Zee AG 2007 Granulosa cell tumors of the ovary: the clinical value of serum inhibin A and B levels in a large single center cohort. *Gynecol Oncol* 105:365–372
- Petraglia F, Luisi S, Pautier P, Sabourin JC, Rey R, Lhomme C, Bidart JM 1998 Inhibin B is the major form of inhibin/activin family secreted by granulosa cell tumors. *J Clin Endocrinol Metab* 83:1029–1032
- Lappöhn RE, Burger HG, Bouma J, Bangah M, Krans M 1992 Inhibin as a marker for granulosa cell tumor. *Acta Obstet Gynecol Scand Suppl* 155:61–65
- Rey RA, Lhomme C, Marcillac I, Lahlou N, Duvillard P, Josso N, Bidart JM 1996 Antimüllerian hormone as a serum marker of granulosa cell tumors of the ovary: comparative study with serum α -inhibin and estradiol. *Am J Obstet Gynecol* 174:958–965
- Young RH, Dickersin GR, Scully RE 1984 Juvenile granulosa cell tumor of the ovary. A clinicopathological analysis of 125 cases. *Am J Surg Pathol* 8:575–596
- Shah SP, Köbel M, Senz J, Morin RD, Clarke BA, Wiegand KC, Leung G, Zayed A, Mehl E, Kalloger SE, Sun M, Giuliany R, Yorlida E, Jones S, Varhol R, Swenerton KD, Miller D, Clement PB, Crane C, Madore J, Provencher D, Leung P, DeFazio A, Khattri J, Turashvili G, Zhao Y, Zeng T, Glover JN, Vanderhyden B, Zhao C, Parkinson CA, Jimenez-Linan M, Bowtell DD, Mes-Masson AM, Brenton JD, Aparicio SA, Boyd N, Hirst M, Gilks CB, Marra M, Huntsman DG 2009 Mutation of FOXL2 in granulosa-cell tumors of the ovary. *N Engl J Med* 360:2719–2729
- Beamer WG, Shultz KL, Tennent BJ, Azumi N, Sundberg JP 1998 Mouse model for malignant juvenile ovarian granulosa cell tumors. *Toxicol Pathol* 26:704–710
- Dorward AM, Shultz KL, Horton LG, Li R, Churchill GA, Beamer WG 2005 Distal Chr 4 harbors a genetic locus (Gct1) fundamental for spontaneous ovarian granulosa cell tumorigenesis in a mouse model. *Cancer Res* 65:1259–1264
- Beamer WG, Tennent BJ, Shultz KL, Nadeau JH, Shultz LD, Skow LC 1988 Gene for ovarian granulosa cell tumor susceptibility, Gct, in SWXJ recombinant inbred strains of mice revealed by dehydroepiandrosterone. *Cancer Res* 48:5092–5095
- Matzuk MM, Finegold MJ, Su JG, Hsueh AJ, Bradley A 1992 α -Inhibin is a tumor-suppressor gene with gonadal specificity in mice. *Nature* 360:313–319
- Matzuk MM, Finegold MJ, Mather JP, Krummen L, Lu H, Bradley A 1994 Development of cancer cachexia-like syndrome and adrenal tumors in inhibin-deficient mice. *Proc Natl Acad Sci USA* 91:8817–8821
- Boerboom D, Paquet M, Hsieh M, Liu J, Jamin SP, Behringer RR, Sirois J, Taketo MM, Richards JS 2005 Misregulated Wnt/ β -catenin

- signaling leads to ovarian granulosa cell tumor development. *Cancer Res* 65:9206–9215
25. Dutertre M, Gouédard L, Xavier F, Long WQ, di Clemente N, Picard JY, Rey R 2001 Ovarian granulosa cell tumors express a functional membrane receptor for anti-Müllerian hormone in transgenic mice. *Endocrinology* 142:4040–4046
 26. Rahman NA, Kananen Rilianawati K, Pauku T, Mikola M, Markkula M, Hämäläinen T, Huhtaniemi IT 1998 Transgenic mouse models for gonadal tumorigenesis. *Mol Cell Endocrinol* 145:167–174
 27. Pangas SA, Li X, Umans L, Zwijsen A, Huylebroeck D, Gutierrez C, Wang D, Martin JF, Jamin SP, Behringer RR, Robertson EJ, Matzuk MM 2008 Conditional deletion of Smad1 and Smad5 in somatic cells of male and female gonads leads to metastatic tumor development in mice. *Mol Cell Biol* 28:248–257
 28. Jorgez CJ, Klysik M, Jamin SP, Behringer RR, Matzuk MM 2004 Granulosa cell-specific inactivation of follistatin causes female fertility defects. *Mol Endocrinol* 18:953–967
 29. Visser JA, Durlinger AL, Peters IJ, van den Heuvel ER, Rose UM, Kramer P, de Jong FH, Themmen AP 2007 Increased oocyte degeneration and follicular atresia during the estrous cycle in anti-Müllerian hormone null mice. *Endocrinology* 148:2301–2308
 30. Pangas SA, Li X, Robertson EJ, Matzuk MM 2006 Premature luteinization and cumulus cell defects in ovarian-specific Smad4 knockout mice. *Mol Endocrinol* 20:1406–1422
 31. Anttonen M, Unkila-Kallio L, Leminen A, Butzow R, Heikinheimo M 2005 High GATA-4 expression associates with aggressive behavior, whereas low anti-Müllerian hormone expression associates with growth potential of ovarian granulosa cell tumors. *J Clin Endocrinol Metab* 90:6529–6535
 32. Salmon NA, Handyside AH, Joyce IM 2004 Oocyte regulation of anti-Müllerian hormone expression in granulosa cells during ovarian follicle development in mice. *Dev Biol* 266:201–208
 33. Münsterberg A, Lovell-Badge R 1991 Expression of the mouse anti-Müllerian hormone gene suggests a role in both male and female sexual differentiation. *Development* 113:613–624
 34. Gustafson ML, Lee MM, Asmundson L, MacLaughlin DT, Donahoe PK 1993 Müllerian inhibiting substance in the diagnosis and management of intersex and gonadal abnormalities. *J Pediatr Surg* 28:439–444
 35. Lane AH, Lee MM, Fuller Jr AF, Kehas DJ, Donahoe PK, MacLaughlin DT 1999 Diagnostic utility of Müllerian inhibiting substance determination in patients with primary and recurrent granulosa cell tumors. *Gynecol Oncol* 73:51–55
 36. Long WQ, Ranchin V, Pautier P, Belville C, Denizot P, Cailla H, Lhommé C, Picard JY, Bidart JM, Rey R 2000 Detection of minimal levels of serum anti-Müllerian hormone during follow-up of patients with ovarian granulosa cell tumor by means of a highly sensitive enzyme-linked immunosorbent assay. *J Clin Endocrinol Metab* 85:540–544
 37. Li Q, Kumar R, Underwood K, O'Connor AE, Loveland KL, Seehra JS, Matzuk MM 2007 Prevention of cachexia-like syndrome development and reduction of tumor progression in inhibin-deficient mice following administration of a chimeric activin receptor type II-murine Fc protein. *Mol Hum Reprod* 13:675–683
 38. Xu J, Oakley J, McGee EA 2002 Stage-specific expression of Smad2 and Smad3 during folliculogenesis. *Biol Reprod* 66:1571–1578
 39. Pangas SA, Rademaker AW, Fishman DA, Woodruff TK 2002 Localization of the activin signal transduction components in normal human ovarian follicles: implications for autocrine and paracrine signaling in the ovary. *J Clin Endocrinol Metab* 87:2644–2657
 40. Lappöhn RE, Burger HG, Bouma J, Bangah M, Krans M, de Bruijn HW 1989 Inhibin as a marker for granulosa-cell tumors. *N Engl J Med* 321:790–793
 41. Robertson DM, Pruysers E, Burger HG, Jobling T, McNeillage J, Healy D 2004 Inhibins and ovarian cancer. *Mol Cell Endocrinol* 225:65–71
 42. Gustafson ML, Lee MM, Scully RE, Moncure AC, Hirakawa T, Goodman A, Muntz HG, Donahoe PK, MacLaughlin DT, Fuller Jr AF 1992 Müllerian inhibiting substance as a marker for ovarian sex-cord tumor. *N Engl J Med* 326:466–471
 43. Baarends WM, Uilenbroek JT, Kramer P, Hoogerbrugge JW, van Leeuwen EC, Themmen AP, Grootegoed JA 1995 Anti-müllerian hormone and anti-müllerian hormone type II receptor messenger ribonucleic acid expression in rat ovaries during postnatal development, the estrous cycle, and gonadotropin-induced follicle growth. *Endocrinology* 136:4951–4962
 44. Weenen C, Laven JS, Von Bergh AR, Cranfield M, Groome NP, Visser JA, Kramer P, Fauser BC, Themmen AP 2004 Anti-Müllerian hormone expression pattern in the human ovary: potential implications for initial and cyclic follicle recruitment. *Mol Hum Reprod* 10:77–83
 45. Teixeira J, Maheswaran S, Donahoe PK 2001 Müllerian inhibiting substance: an instructive developmental hormone with diagnostic and possible therapeutic applications. *Endocr Rev* 22:657–674
 46. Visser JA, Themmen AP 2005 Anti-Müllerian hormone and folliculogenesis. *Mol Cell Endocrinol* 234:81–86
 47. Donahoe PK, Clarke T, Teixeira J, Maheswaran S, MacLaughlin DT 2003 Enhanced purification and production of Müllerian inhibiting substance for therapeutic applications. *Mol Cell Endocrinol* 211:37–42
 48. Masiakos PT, MacLaughlin DT, Maheswaran S, Teixeira J, Fuller Jr AF, Shah PC, Kehas DJ, Kenneally MK, Dombkowski DM, Ha TU, Pfeffer FI, Donahoe PK 1999 Human ovarian cancer, cell lines, and primary ascites cells express the human Müllerian inhibiting substance (MIS) type II receptor, bind, and are responsive to MIS. *Clin Cancer Res* 5:3488–3499
 49. Choi KC, Kang SK, Nathwani PS, Cheng KW, Auersperg N, Leung PC 2001 Differential expression of activin/inhibin subunit and activin receptor mRNAs in normal and neoplastic ovarian surface epithelium (OSE). *Mol Cell Endocrinol* 174:99–110
 50. Di Simone N, Crowley Jr WF, Wang QF, Sluss PM, Schneyer AL 1996 Characterization of inhibin/activin subunit, follistatin, and activin type II receptors in human ovarian cancer cell lines: a potential role in autocrine growth regulation. *Endocrinology* 137:486–494
 51. Steller MD, Shaw TJ, Vanderhyden BC, Ethier JF 2005 Inhibin resistance is associated with aggressive tumorigenicity of ovarian cancer cells. *Mol Cancer Res* 3:50–61
 52. Pieretti-Vanmarcke R, Donahoe PK, Pearsall LA, Dinulescu DM, Connolly DC, Halpern EF, Seiden MV, MacLaughlin DT 2006 Müllerian inhibiting substance enhances subclinical doses of chemotherapeutic agents to inhibit human and mouse ovarian cancer. *Proc Natl Acad Sci USA* 103:17426–17431
 53. Bittinger S, Alexiadis M, Fuller PJ 2009 Expression status and mutational analysis of the PTEN and P13K subunit genes in ovarian granulosa cell tumors. *Int J Gynecol Cancer* 19:339–342
 54. Nasu K, Fukuda J, Yoshimatsu J, Takai N, Kashima K, Narahara H 2007 Granulosa cell tumor associated with secondary amenorrhea and serum luteinizing hormone elevation. *Int J Clin Oncol* 12:228–230
 55. Fuller PJ, Chu S, Fikret S, Burger HG 2002 Molecular pathogenesis of granulosa cell tumours. *Mol Cell Endocrinol* 191:89–96
 56. Merras-Salmio L, Vetteranta K, Möttönen M, Heikinheimo M 2002 Ovarian granulosa cell tumors in childhood. *Pediatr Hematol Oncol* 19:145–156